Food Bioprocess Technol (2016) 9:1674–1680
DOI 10.1007/s11947-016-1751-9

ORIGINAL PAPER

Opacity Studies in Dehydrated Fruits in Relation to Proton Mobility and Supramolecular Aspects

Lina M. Agudelo-Laverde[1,2] · **Nuria Acevedo**[1,3] · **Carolina Schebor**[1] · **María del Pilar Buera**[1]

Received: 23 July 2015 / Accepted: 30 May 2016 / Published online: 3 June 2016

Abstract Water content is one of the variables affecting light scattering in foods, which on time determine gloss, translucence, and transparency. The objective of this study was to evaluate the effect of freeze-drying, humidification, and storage time on the changes of light distribution inside fruit tissues and their relationship with glass transition and proton mobility. Sliced and powdered freeze-dried apple, pear, and melon humidified at different relative humidities were employed. All the studied materials were translucent when fresh and became opaque after the freeze-drying process. In freeze-dried sliced fruits, the cellular structure contributed to maintain air inside the matrices, and then the opacity of the materials was almost constant, independently of the relative humidity. In the powdered materials, the compacted structure retained less air than sliced samples, and the powders were translucent due to the lower number of light-matter interfaces than in the porous-dried fruits, leading to a lower internal diffusion. The opacity decrease when increasing the water mass fraction followed a variation parallel to the T_g curve. Opacity decrease occurred at $T\text{-}T_g$ values above 38 °C and was coincident with the observation of a proton population of higher mobility than that observed below the water content hydration limit value. Proton mobility at a molecular scale could thus be related to supramolecular events affecting food appearance, and this information may help to develop food products with the desired appearance.

Keywords Opacity · Freeze-dried fruits · Glass transition · Nuclear magnetic resonance · Humidification

María del Pilar Buera and Carolina Schebor are Members of FCEN-UBA, CONICET, Buenos Aires, Argentina.

✉ María del Pilar Buera
pilar@di.fcen.uba.ar

[1] Departamento de Industrias, Facultad de Ciencias Exactas y Naturales, Universidad de Buenos Aires, (FCEyN-UBA), CONICET, Buenos Aires, Argentina

[2] Present address: Universidad del Quindío, Armenia, Colombia

[3] Present address: Food Sciences Building, Iowa State University, Ames, Iowa, USA

Introduction

Non-chromatic characteristics derived from the interaction of light with matter lead to the opaque/translucent/transparent and glossy/matte characteristics of the materials and greatly affect color perception. Transparent materials do not change the direction of incident radiation, while in opaque samples the flux of light cannot pass through them; as an intermediate type between opaque and transparent materials, inside translucent bodies light is transmitted and reflected in different directions to the incident flow, giving rise to scattering phenomena (Hutchings et al. 2013; MacDougall 2010, 2002; Lozano 1978). Translucency is a critical property of many foods and drinks and affects the consumer perception of volume and texture. The visual appearance produced by the different spatial distributions of light has been called "cesia" (Caivano 1991). An atlas of cesia was developed, which has been useful for different applications like paintings development, architecture, and materials for ambient illumination (Caivano et al. 2004; Caivano 1996, 1994, 1991). While the chromatic properties characterize the color of a certain object by means of three variables (hue, saturation, and luminosity), cesia shares the lightness coordinate with the chromatic properties but includes the variables permeability (which defines the transparent/opaque scale) and diffusivity (which defines

the glossy/matte characteristics) (Caivano et al. 2004; Caivano 1996, 1994, 1991).

Lighting properties, such as spectral intensity, directional distribution, and color rendering ability, also affect the perceived color, gloss, and translucency of objects (McDougall 2002). Water content is one of the main variables affecting light scattering, since it determines structural properties, the extent and kinetics of changes such as those derived from glass transitions and crystallization, which impact gloss and transparency. In the light path inside the materials, refractive index changes (due to phase separation, bubbles formation, suspended solid particles, or emulsion drops) affect food appearance attributes and visual texture. Since the interaction of light with matter depends on the sample structure and also on dynamic aspects, ^{1}H-NMR relaxation times could be employed to establish a direct relationship with the opacity changes. Nuclear magnetic resonance (NMR) technique is employed to characterize the mobility of water and solids in food systems (Schmidt 2004).

Due to the relationship among structural attributes, water content, and food appearance, the construction of state diagrams is an effective tool to predict the changes of food materials appearance during food processing and storage (Bazardeh and Esmaiili 2014; Bhandari and Howes 1999; Roos 1993).

Although a correlation between translucency and sugar accumulation has been described for dried pineapple (Chen and Paull 2001), no studies have been previously performed on the relationship of the opacity and glass transition phenomena in freeze-dried fruits. Therefore, the objective of this study was to evaluate the effect of humidification on opacity changes in freeze-dried sliced and powdered fruits and their relationship with the glass transition phenomenon and proton mobility.

Materials and Methods

Materials Preparation

Fully ripe fresh apples (Granny Smith), melons (Honeydew), and pears (Packam's Triumph) were obtained from the local market in Buenos Aires, Argentina, and stored at 4 °C for up to 3 days. The fruits were washed, peeled, and transversally cut into cylindrical slices (1.5 cm diameter and 0.5 cm thickness). The slices were immediately frozen with liquid nitrogen (−190 °C) in order to form small ice crystals (Voda et al. 2012; Kiani and Sun 2011) and fast inhibiting enzymatic reactions (Acevedo et al. 2008), and stored at −20 °C for 24 h. Before freeze-drying, 2 kg of previously frozen fruit slices were covered again with liquid nitrogen for favoring complete ice crystallization. The freeze-drier (ALPHA 1-4 LD2 Martin Christ Gefriertrocknungsanlagen GMB, Germany) was operated with a condenser plate at −55 °C, at a chamber pressure of 4 Pa, and the process last 48 h. After freeze-drying, around 1 kg of fruit were powdered employing an electric coffee grinder (Braun, Germany). Sliced and powdered samples were distributed into vials for humidification. Freeze-dried cylindrical slices were employed for determination of water content and thermal transitions. Both sliced and powdered samples were re-humidified over saturated salt solutions (in a range of 11–84 % RH) in vacuum desiccators for 14 days at 25 °C (Greenspan 1977). After equilibration, the cylinders and powder fruit were located in six rubber o-rings (2.5 cm internal diameter) between two glass plates hermetically sealed. The rubber o-rings formed the sample holders walls avoiding water loss (Acevedo et al. 2008). Then the sample holders were stored in a forced air oven at 45 ± 1 °C for 15 days. The glass plates (containing six fruit slices or six powdered samples) were removed at certain time intervals (1, 2, 4, 6, 8, 10, and 15 days), the images were captured and the samples placed back in the oven.

Water Content

The water content was determined gravimetrically by weight difference before and after vacuum drying over magnesium perchlorate at 70 °C for 48 h. An average value of at least two replicates was reported along with the standard deviation.

Thermal Transitions

Glass transitions were determined by differential scanning calorimetry (DSC; onset values) using a DSC 822e Mettler Toledo calorimeter (Schwerzenbach, Switzerland). The instrument was calibrated with pure milli-Q water (0 °C), indium (156.6 °C), lead (327.5 °C), and zinc (419.6 °C). All measurements were performed at a heating rate of 10 °C/min. Hermetically sealed 40-μl medium pressure aluminum pans were used, (an empty pan served as a reference). Thermograms were evaluated using STAR^{e} software v.6.1 Mettler Thermal Analysis (Mettler Toledo, Schwerzenbach, Switzerland).

Proton Mobility

Time resolved proton nuclear magnetic resonance (^{1}H NMR) was employed to determine the transversal or spin–spin relaxation times (T_2) (Kirtil and Oztop 2016). A Bruker Minispec mq20 (Bruker Biospin Gmbh, Rheinstetten, Germany) which operates at 0.47 T magnetic field and at a resonance frequency of 20 MHz was used. Humidified fruits were removed from the desiccators placed into 10-mm diameter glass tubes and returned to the desiccators for additional 24 h prior to analysis. All determinations were performed in triplicate at 25 °C. The average and standard deviation are reported.

Proton populations of different mobility were measured using Hahn spin-echo sequence. The method consists of a (90° - τ - 180°) sequence (Demco et al. 2013; Farroni and Buera 2014; Hahn 1950). This method is associated with slow relaxing protons (related to the populations of water molecules displaying less interaction with solids). Freeze-dried fruits humidified between 11 and 84 % RH were analyzed using this sequence. The following settings were used: scans = 4, recycle delay = 1.5 s, gain = 75 dB, number of points = 20, time for decay curve display = 2 s, and interpulse (τ) range of 0.001–2 ms. The interpulse range was selected in order to record the complete relaxation of the signal. No phase cycling was used. A polyvinylpyrrolidone (PVP of 58,000 Da) system equilibrated at 52 % RH was used for the automatic update of the equipment which tunes the pulse duration, detection angles, gain, and magnetic field homogeneity.

The decay envelopes obtained after Hahn pulse sequence applied were fitted to bi-exponential behavior with the following equation:

$$I = A_1 \exp(-t/T_{2-1}) + A_2 \exp(-t/T_{2-2})$$

where I represents the NMR signal intensity at time t. The relaxation time T_{2-1} corresponds to the protons in the less mobile water fraction for each sequence employed. A_1 is proportional to the number of protons in the T_{2-1} state. The relaxation time T_{2-2} corresponds to the more mobile water fraction. A_2 is proportional to the number of protons in the T_{2-2} state.

Opacity Measurements

Fruits translucence changes were determined by opacity measurements through image analysis. The computer vision system (CVS) employed to study the optical properties, previously described by Agudelo-Laverde et al. (2014a) allowed acquiring information for all six samples directly inside each glass plate and then calculating an average color for the entire image. L*, a*, and b* color coordinates were obtained by converting the data from Adobe Photoshop CS4 (Adobe Systems Inc., San Jose, CA) program to the CIELAB color space (Papadakis et al. 2000). Freeze-dried and humidified samples were transferred from the forced air oven to the gray box, and images were acquired at different times (between 1 and 15 days) during storage.

In order to analyze the opacity change of solid matters, without the interference air, freeze-dried samples were powdered and compacted, and the behavior of both powders and slices was studied. Powdered samples presented different opacity degrees, which was calculated by the ratio between the L* values obtained for black and white backgrounds. An opacity value of 1 corresponds to an opaque sample, while lower values correspond to different translucency degrees. An average value of six replicates was reported along with the standard deviation.

$$\text{Opacity} = \frac{L^*\ \text{black background}}{L^*\ \text{white background}}$$

In order to compare the opacity of slices and powders, samples with the same thickness (3 mm) were analyzed. Thus, it was necessary to employ about the double amount of powdered fruit in the compacted samples (0.38 ± 0.07 g) than in the slices (0.19 ± 0.03 g) to complete the o-ring space, which means that the air inside slices occupied around 50 % of their volume (Mayor et al. 2011).

Results and Discussion

Effect of Freeze-Dying Process on Material Opacity

Slices of all fruits studied were translucent when fresh and became opaque after the freeze-drying process (Fig. 1). The opacity changes can be analyzed by quantifying the ratio of the samples reflectance measured with black and white background.

At the studied sample thickness values, dehydrated samples showed opacity values close to 1 (Fig. 2). Differences in the opacity values of fresh and dried fruits can be explained by the differences in light dispersion inside the material. In the fresh tissues, the inter- and intra-cellular spaces are filled with water. Upon freeze-drying, cellular spaces left by ice sublimation are replaced by air. When the light passes through the dried material, it suffers multiple reflections and refractions and it is dispersed through diffusional phenomena, due to the differences in the refraction index between the solid matter (n about 1.5) and air (n = 1) (Saarela et al. 2008). As the difference of refractive index between solids and water (n = 1.33) is smaller than that between solids and air, fresh fruit slices showed lower opacity values (between 80 and 90 %) and they behave as translucent.

Effect of Humidification on Opacity Degree

The influence of re-humidification of dry samples on optical properties was analyzed in sliced and powdered samples (Fig. 3). In freeze-dried slices, the opacity was almost constant, close to unit, independently of the RH value. On the other side, in the powdered materials, opacity decreased as increasing relative humidity from 22 % in apple and from 33 % in melon and pear. It is interesting to note that the translucent behavior appeared in the powdered and compacted samples at lower RH values lower than 0.75, at which water

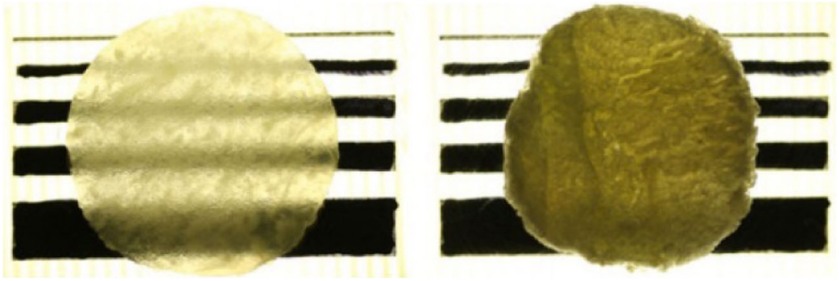

Fig. 1 Retro-illuminated images of fruit slices, the image on the left corresponds to the fresh fruit and that on the right corresponds to the freeze-dried sample. The *black lines* in the back are no longer seen in the freeze dried material due to the water replace for air

fill the pores of vegetable materials and capillary condensation occurs (Lana et al. 2006; Talens et al. 2002).

While not related to capillary filling, the translucent appearance could be explained by the samples storage at temperatures higher than T_g (up to T-T_g > 38 °C) that promoted structural shrinkage and stickiness. The T-T_g values for the samples at which opacity started to decrease are indicated in shaded circles in Fig. 3. It was previously reported that at the RH corresponding to perceived opacity in present work, structural collapse also takes place (Agudelo-Laverde et al. 2014a).

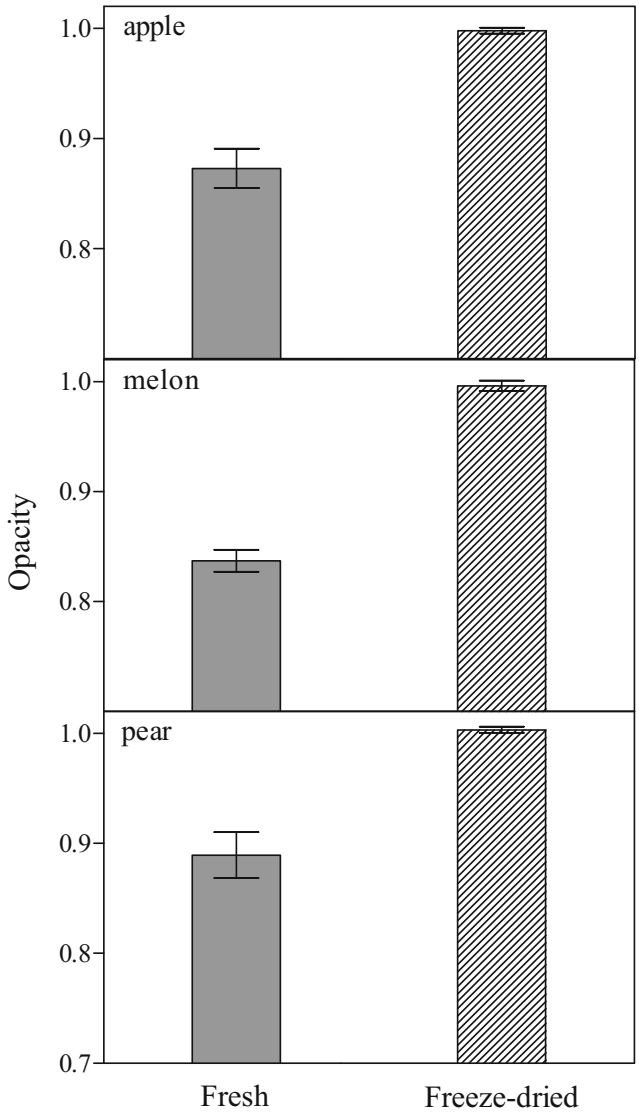

Fig. 2 Opacity percentage of fresh and freeze-dried apple, melon, and pear slices. Data are expressed as mean values and standard deviations of six replicates

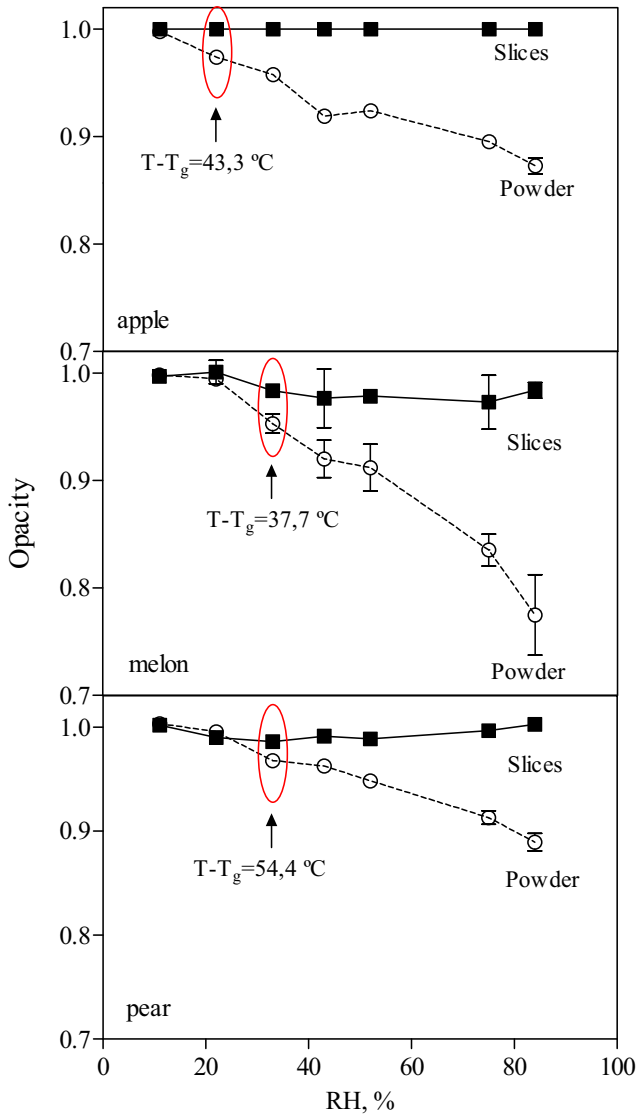

Fig. 3 Opacity degree for apple, pear, and melon in slices (*full symbols*) and powder (*open symbols*) as a function of RH, after 14 days of humidification time at 25 °C. T-T_g values correspond to the point at which the opacity decrease started. Data are expressed as mean values and standard deviations of six replicates

Table 1 Relaxation times of different proton populations determined by NMR after Hahn pulse sequence in freeze-dried fruit samples humidified at 33 % RH

Sample	T_{2-1} (ms)	T_{2-2} (ms)
Apple	0.05 ± 0.01	0.31 ± 0.03
Melon	0.05 ± 0.01	0.44 ± 0.05
Pear	0.07 ± 0.01	0.32 ± 0.02

It has been previously reported that in several dried fruits the inverse of the transverse relaxation time obtained by NMR remained almost constant up to 33 % RH (Agudelo-Laverde et al. 2014b) and then increased. While below 33 % RH only the proton populations with shorter relaxation times (0.05 ± 0.02 ms) were detected, two proton populations with different mobility, called T_{2-1} and T_{2-2}, respectively, were observed in the studied fruits samples at RH 33 % after the Hahn pulse sequence application. Table 1 summarizes relaxation times obtained. It is important to note that the material opacity started to decrease at the same RH at which the second proton population was observed, as detected by the Hahn sequence. The first proton population, with shorter relaxation times, is related to water strongly interacting with the solids present in the material. When the water content was higher than this limit and the most active sites of the material were saturated, water mobility started to increase, and then opacity loss was observed.

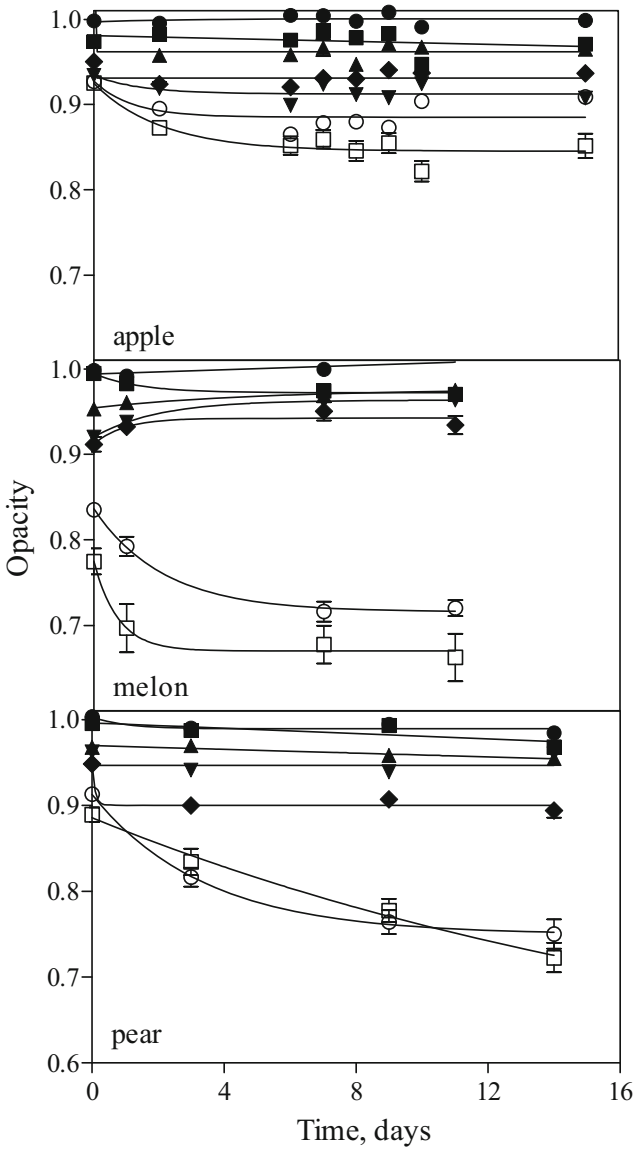

Fig. 4 Opacity degree of apple, melon, and pear humidified at 11 (*black circle*), 22 (*black square*), 33 (*black triangle*), 43 (*black down-pointing triangle*), 52 (*black diamond*), 75 (*white circle*), and 84 % (*white square*) RH as a function the storage time at 45 °C. Data are expressed as mean values and standard deviations of six replicates

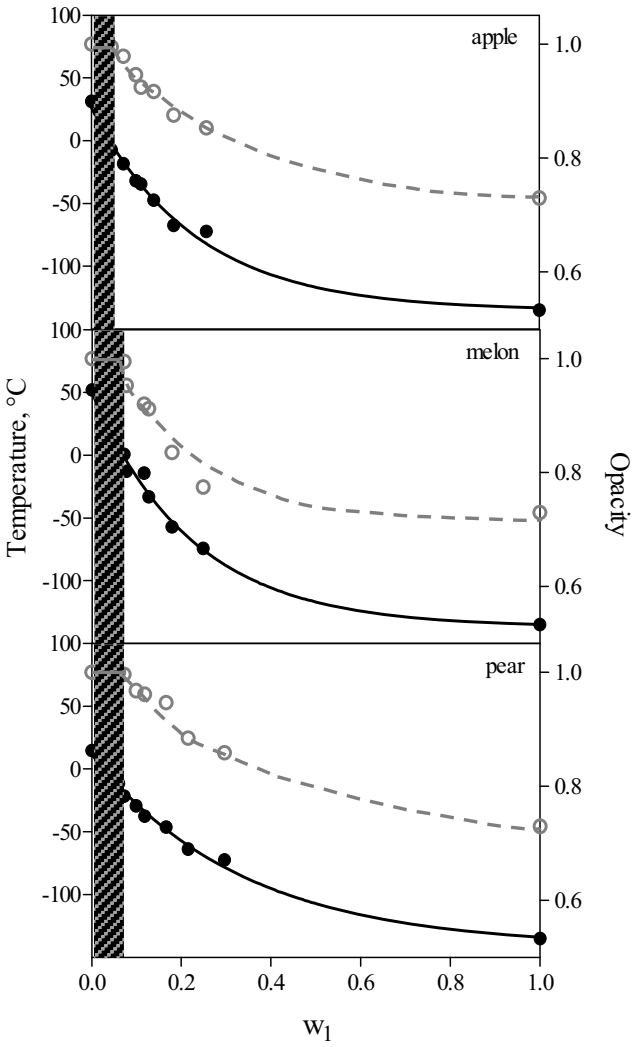

Fig. 5 Glass transition temperature (*continuous lines*) and opacity degree of apple, melon, and pear (*dashed lines*) as a function the mass fraction of water (w_1). The *shaded zone* corresponds to opaque behavior

Effect of Storage Time on Opacity Degree of Freeze-Dried Fruits

Opacity of freeze-dried fruits was studied during storage time at 45 °C. As shown in Fig. 4, at low relative humidities (11, 22, 33 % RH), no important changes of the opacity of freeze-dried slices were detected during storage. At intermediate RH values (43, 52 % RH), opacity degree changes were observed only initially ($t = 0$), indicating that the translucence changes were generated by humidification, but opacity degree did not change during storage. On the other hand, when the materials were humidified at high relative humidities (75 % and higher), the opacity values decreased during storage at 45 °C. Apple samples presented the lowest opacity changes during storage, while melon and pear showed an important opacity decrease. While melon samples were the most affected by humidification stage at 75 and 84 % RH (corresponding to storage time = 0), pear samples were still opaque after humidification at these RH and showed the main decrease of opacity values during storage time at 45 °C.

Figure 5 shows the glass transition temperature (T_g) of the samples and the corresponding opacity degree plotted as a function mass fraction of water (w_1) corresponding to a RH range between 11 and 84 % for apple, melon, and pear. The shaded area in Fig. 5 corresponds to the opaque behavior of the samples. At w_1 values lower than 0.1, the samples behave as opaque materials, with opacity values constant and close to unity. At mass fractions of water higher than 0.1, a parallel behavior between opacity decrease and T_g was observed in all studied fruits as a function of w_1, which is coincident with the translucent behavior. It is important to note that the parallelism between opacity decrease and glass transition temperatures as a function of water content has not been previously reported, and demonstrates the high impact of the glass transition in food structure and appearance.

Conclusions

In freeze-dried fruits at water mass fraction below 0.1, the light diffusional phenomenon promoted by the multiple reflections in compartmentalized media of different refractive index lead to the opaque behavior of the samples.

Freeze-dried fruit slices behave as opaque materials, with opacity close to unit, independently of the RH value. On the other side, in the powdered materials, opacity decreased as increasing relative humidity from RH values between 22 and 33 %. The translucent behavior occurred at RH values lower than the corresponding to capillary condensation. The opacity decrease (giving place to translucence) occurred at T-T_g values above 38 °C and was coincident with the observation of a second proton population of higher mobility than that below the water content hydration limit value. Above the water mass fraction of 0.1, the opacity and T_g decrease followed parallel variation with increasing the mass fraction of water.

Thus, the macroscopic food appearance could be related to proton mobility taking place at a molecular scale and to supramolecular events manifested by the relationship of the glass transition dependence with the water content.

Acknowledgments The authors acknowledge financial support from UBACYT 20020130100443BA and ANPCYT (PICT-2013 1331).

References

Acevedo, N., Briones, V., Buera, M., & Aguilera, J. (2008). Microstructure affects the rates of chemical, physical and color changes during storage of dried apple discs. *Journal of Food Engineering, 85*(2), 222–231.

Agudelo-Laverde, L. M., Schebor, C., & Buera, M. P. (2014a). Evaluation of structural shrinkage on freeze-dried fruits by image analysis: effect of relative humidity and heat treatment. *Food and Bioprocess Technology, 7*(9), 2618–2626.

Agudelo-Laverde, L. M., Schebor, C., & Buera, M. P. (2014b). Proton mobility for the description of dynamic aspects of freeze-dried fruits. *Journal of Food Engineering, 125*, 44–50.

Bhandari, B. R., & Howes, T. (1999). Implication of glass transition for drying and stability of dried foods. *Journal of Food Engineering, 40*, 71–79.

Bazardeh, M. E., & Esmaiili, M. (2014). Sorption isotherm and state diagram in evaluating storage stability for sultana raisins. *Journal of Stored Products Research, 59*, 140–145.

Caivano, J. (1991). Cesia: a system of visual signs complementing color. *Color Research and Application, 16*(4), 258–268.

Caivano, J. L. (1994). Appearance (cesia): construction of scales by means of spinning disks. *Color Research and Application, 19*, 351–362.

Caivano, J. L. (1996). Cesia: its relation to color in terms of the trichromatic theory. *Die Farbe, 4*(1/3), 51–63.

Caivano, J.L., Menghi, I., & Iadisernia, N. (2004). Cesia and paints: an atlas of cesia with painted samples. AIC 2004 Color and Paints, Interim Meeting of the International Color Association, Proceedings.

Chen, C. C., & Paull, R. E. (2001). Fruit temperature and crown removal on the occurrence of pineapple fruit translucency. *Scientia Horticulturae, 88*, 85–95.

Demco, D. E., Oros-Peusquens, A. M., Utiu, L., Fechete, R., Blümich, B., & Jon Shah, N. (2013). Molecular dynamics parameter maps by 1H Hahn echo and mixed-echo phase-encoding MRI. *Journal of Magnetic Resonance, 227*, 1–8.

Farroni, A. E., & Buera, M. P. (2014). Cornflake production process: state diagram and water mobility characteristics. *Food and Bioprocess Technology, 7*, 2902–2911.

Greenspan, L. (1977). Humidity fixed points of binary saturated aqueous solutions. *Journal of Research, 8*, 89–96.

Hahn, E. L. (1950). Spin echoes. *Physical Review, 80*(4), 580–594.

Hutchings, J. B., Ronnier Lou, M., & Ji, W. (2013). *Food appearance quality assessment and specification in: instrumental assessment of food sensory quality, a practical guide*. Cambrige UK: Woodhead Publishing.

Kiani, H., & Sun, D. W. (2011). Water crystallization and its importance to freezing of foods: a review. *Trends in Food Science & Technology, 22*, 407–426.

Kirtil, E., & Oztop, M. H. (2016). 1H nuclear magnetic resonance relaxometry and magnetic resonance imaging and applications in food science and processing. *Food Engineering Reviews, 8*, 1–22.

Lana, M. M., Tijskens, L. M. M., & Kooten, O. (2006). Modelling RGB colour aspects and translucency of fresh-cut tomatoes. *Postharvest Biology and Technology, 40*, 15–25.

Lozano, R. (1978). *El color y su medición*. Buenos Aires: Editorial América Lee.

MacDougall, D. B. (2002). In MacDougall (Ed.), *Colour in food improving quality*. Boca Ratón: CRC Press.

MacDougall, D. B. (2010). Color measurement. In *Principles, advances and industrial applications*. Cambrige: Woodhead Publishing.

Mayor, L., Moreira, R., & Sereno, A. M. (2011). Shrinkage, density, porosity and shape changes during dehydration of pumpkin (*Cucurbita pepo L.*) fruits. *Journal of Food Engineering, 103*, 29–37.

Papadakis, S., Abdul-Malek, S., Kandem, R., & Yam, K. (2000). A versatile and inexpensive technique for measuring colour of foods. *Food Technology, 54*(12), 48–51.

Roos, Y. H. (1993). Water activity and physical state effects on amorphous food stability. *Journal of Food Processing and Preservation, 16*(6), 433–447.

Saarela, J. M. S., Heikkinen, S. M., Fabritius, T. E. J., Haapala, A. T., & Myllylä, R. A. (2008). Refractive index matching improves optical object detection in paper. *Measurement Science and Technology, 19*, 1–7.

Schmidt, S. J. (2004). Water and solid mobility in foods. *Advances in Food and Nutrition Research, 48*, 1–101.

Talens, P., Martínez-Navarrete, P., Fito, N., & Chiralt, A. (2002). Changes in optical and mechanical properties during osmodehydrofreezing of kiwi fruit. *Innovative Food Science & Emerging Technologies, 3*, 191–199.

Voda, A., Homan, N., Witek, M., Duijster, A., van Dalen, G., van der Sman, R., et al. (2012). The impact of freeze-drying on microstructure and rehydration properties of carrot. *Food Research International, 49*, 687–693.